Determination of Post Mortem Human Subject Response to Vertical Drop Tower Testing and Initial Application for Total Human Model For Safety Finite Element Model Validation

T. R. DeWitt[1], A. M. Marcallini[1], J. H. Bolte[1] and Y. S. Kang[1]
[1] The Ohio State University

ABSTRACT

Drop tower testing was conducted using 50th percentile male PMHS at 15G peak acceleration in a rigid seat, with a seatpan-to-seatback angle of 90°. Subjects were instrumented with 6DOF motion blocks at T1, T4, T12, L3, and S1 to capture detailed vertebral body kinematics. Pressure sensors were also placed throughout the lumbar spine to estimate force in the intervertebral discs from S1-L2. PMHS were restrained using a pilot torso harness attached to the seat at the shoulders and lap belt, both pretensioned to 89N. Reaction forces were measured in the seat using six-axis loads under the seatpan. Final positioning of the occupant was documented using a FARO arm point probe and laser scanner. To recreate the experimental setup, CAD models of the experimental fixture were meshed using a commercial FE modeling software (Hypermesh) and imported into LS-Dyna for incorporation with the THUMS model. The belt routing tool in LS-PrePost v4.9.12 was used to develop the torso harness and shoulder and lap belts. Pre-simulation was performed to position the THUMS model in accordance with recorded FARO data, and the experimentally recorded seat vertical acceleration was assigned using Boundary_Prescribed_Motion. Finally, instrumentation locations were duplicated within the THUMS model to match the PMHS experimental setup. The THUMS model showed similar head kinematics compared to the experiment, which went first into extension, followed by flexion during the primary pulse. The torso of the model, however, experienced an increased flexion/compression response compared to PMHS. Peak reaction force in the simulated seat load cells measured 12.7kN, which was within one standard deviation of the average normalized experimental values (average = 12.8kN, standard deviation = 0.4kN). Average load in the lumbar spine in the model was found to be 3.3kN, which was lower than PMHS average by more than two standard deviations.

INTRODUCTION

Aircraft ejection seats have been around since the early 1940s with modern variants having been developed as early as the 1970s for some aircraft still in service (Parate et al., 2022). Typical performance for modern seats includes a catapult phase to propel the pilot away from the aircraft, followed by a brief period of free flight and deployment of a recovery parachute. Once the recovery parachute is inflated, the restraint system holding the pilot in the seat is released, and the pilot is allowed to separate from the seat. While a potential for injury exists during all phases of ejection seat operation, the highest potential for compressive spinal injury occurs during the catapult phase when the occupant is rapidly accelerated upwards out of the cockpit and away from the aircraft (Auffret et al., 1975). Depending on the ejection seat model in use, this acceleration can vary from

This paper is a student paper from the 19th Injury Biomechanics Symposium and is published in a special issue of SAE International Journal of Transportation Safety.
It is preliminary work, has not been peer reviewed, and should not be cited because it is a work in progress.

9 to 18G peak with a duration as long as 300ms (Pellettiere et al., 2013). A recent study looking at ejection in the German Armed Forces from 1975 to 2021 revealed the prevalence of spinal injury to be 56% and spine fracture 33% for pilots who have ejected. Of the sixty-six cumulative fractures that were recorded, 89% occurred in either the thoracic or lumbar spine (Sommer et al., 2023). However, a similar study looking at United States Air Force (USAF) ejections between 1981 and 1996 found the prevalence of all major injuries of the head, neck, and spine to be between 2-25% (Collins et al., 1997). Although no details were available on the specific injuries found during the study, there is still a notable difference in the identified injury frequency. Previous studies have shown the number of ejections within the USAF to be as high as 10-50 per year (Collins et al., 1997), and the average cost per pilot for adequate training of aircraft operation can range from $5.6-10.9 million (Mattock et al., 2019). With manned aircraft still being developed and programs currently underway to upgrade legacy ejection seat systems to more modern variants (Harper, 2019), it is important to ensure we understand the factors that contribute to the injury potential of these systems during operation to ensure the safety of the occupants when used and that they can continue to fly after the event.

For ejection seats to be determined safe for use by the United States Department of Defense as well as many of its partner nations, it must go through the Airworthiness process for approval (DODIG-2015-090). This process in done in accordance with MIL-HDBK-516, which outlines requirements for a variety of aircraft systems including ejection seats and requires specific acceleration limits be imposed to ensure the safety of operation and evaluation of these limits using experimentation with instrumented anthropomorphic test devices (ATDs) (EZFC-CSB-16-001). The tests required to produce these data for a qualification program have been estimated at $16M (Thompson, 2019), and methods have gone largely unchanged for nearly three decades. Finite element (FE) human body models (HBMs) have grown in popularity within the automotive industry for safety system performance evaluation (Katagiri et al., 2016, Decker et al., 2019, Gepner et al., 2022). Auto manufacturers have invested heavily in the development of this type of modeling capability to decrease the resources required during system development and provide supplemental data to complement physical research using ATDs or PMHS. The Toyota Total Human Model for Safety (THUMS) AM50 v6.1 has been validated for various frontal, rear, and side impact conditions, but it lacks a detailed validation in a vertical accelerative environment (THUMS AM50 Version 6.1 Users' Manual). The purpose of this study is to utilize a preliminary data set from three 50th percentile male post-mortem human subject (PMHS) tests to provide an initial look at the THUMS capability for use in an ejection-like loading environment.

METHODS

PMHS Testing

Three approximate 50th percentile PMHS were obtained through the Ohio State Body Donation Program and screened to ensure appropriate bone mineral density and the absence of spine abnormalities using Dual-Energy X-ray Absorptiometry (DEXA) and Computed Tomography (CT). To record subject spinal kinematics, six degrees of freedom (6DOF) motion blocks (6DX, DTS, Seal Beach, CA, USA) were rigidly fixed to vertebral bodies at T1, T4, T12, L3, and S1. Pressure sensors (Model 060, Precision Measurements Co, Atlanta GA, USA) were inserted into the center of the intervertebral discs at L2-L3, L3-L4, L4-L5, and L5-S1 to record

This paper is a student paper from the 19th Injury Biomechanics Symposium and is published in a special issue of SAE International Journal of Transportation Safety.
It is preliminary work, has not been peer reviewed, and should not be cited because it is a work in progress.

pressure changes in the lumbar spine, which were used to estimate force in the lumbar spine using area measurements derived from PMHS CT. After the installation of the instrumentation was completed, the instrumentation orientations were recorded using pre-test CT for each subject. Exemplar 6DOF mount and pressure sensor installation are shown in Figure 1.

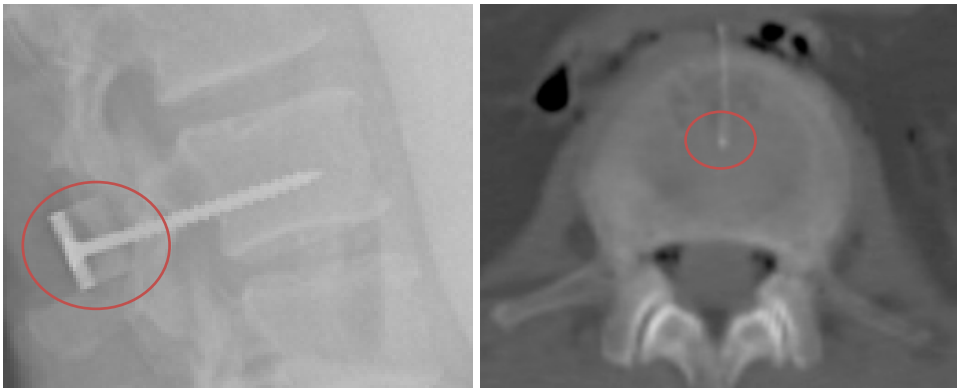

Figure 1: 6DOF vertebral body mount (left) and intervertebral disc pressure sensor (right).

Testing was conducted using the Vertical Drop Tower (VDT) facility at Wright-Patterson Air Force Base, Dayton, Ohio. The facility is composed of a carriage connected to two, fifteen-meter vertical guide rails. The carriage allows for attachment of various seat systems and is raised up the tower to a pre-determined height for testing. The carriage is released and allowed to free fall into a water brake system at the bottom of the tower, producing an accelerative pulse while bringing the carriage to a halt. All testing was conducted at a peak acceleration of 15G, using a rigid seat with a ninety-degree seatpan-to-seatback angle. The PMHS were restrained using a pilot torso harness (PCU-15/P) that was connected to the seat fixture at the shoulders. An additional lap belt was also anchored to the floor of the fixture and around the PMHS. Accelerometers were placed on the carriage to record linear acceleration in the z-axis. Six-axis load cells were placed underneath the seat pan to measure seat reaction force. Single-axis belt load cells were also placed on the belts connecting to the shoulders of the torso harness to measure the tensile force on the restraint system. The torso harness was fit to the PMHS by a trained aircrew flight equipment specialist, and both the shoulder belt and lap belt restraints were pre-tensioned to 89 ± 22N before testing.

PMHS were positioned such that the femora were parallel with the horizontal, and the tibiae and femora were at a relative ninety-degree angle. The head of the PMHS was suspended in an upright position with the Frankfort plane at approximately zero degrees with respect to the horizontal using restraints designed to fail at sub-impact levels. Documentation of the final position for each PMHS was performed using three-dimensional (3D) digitization of anatomical landmarks with a FARO arm device (Edge FaroArm, Faro Arm Technologies, Lake Mary, FL, USA). PMHS were also scanned using an Artec Leo 3D scanner (Artec Leo, Artec 3D Santa Clara, CA) for further documentation on PMHS and fixture positioning and setup. In-position X-ray images were taken to document initial spine curvature during testing. The facility and final setup for PMHS2 can be seen in Figure 2.

This paper is a student paper from the 19th Injury Biomechanics Symposium and is published in a special issue of SAE International Journal of Transportation Safety.
It is preliminary work, has not been peer reviewed, and should not be cited because it is a work in progress.

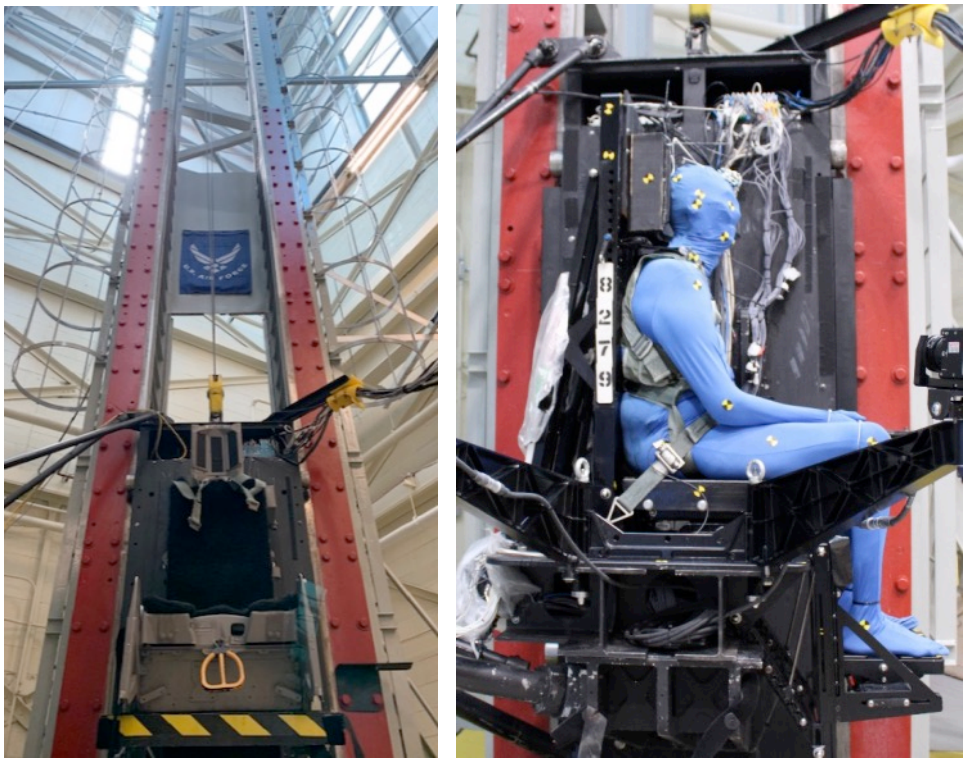

Figure 2: VDT (left) and final PMHS setup (right).

Carriage instrumentation, 6DOF, and pressure sensor data were collected using two on-board data acquisition systems (SlicePro, DTS, Seal Beach, CA, USA), collecting at 20,000 Hz with a 4,000 Hz anti-aliasing filter. High-speed video was recorded using two on-board and one off-board cameras, collecting at 1,000 frames per second. All data were processed in accordance with SAE-J211 [SAE Standard J211-1, 2014] and all PMHS 6DOF data were transformed to the local anatomical coordinate system (Slykhouse et al., 2019) for reporting. This initial evaluation, however, will only focus on vertebral body local anatomical z-acceleration, y-angular velocity, and lumbar force estimates.

Simulation Development

The experimental seat fixture was developed using CAD data from the facility fixture development. Geometries for the fixture were reduced to include only critical components, and features were simplified for FE model creation. All components in the seat model are assumed rigid, with the exception of four load cell components under the seat, which measure seat reaction forces. CAD data were not available for the headrest of the seat fixture model, so this component geometry was reverse-engineered using data obtained from the Artec 3D scanner. This process is summarized in Figure 3. The restraint system model to represent the torso harness, lap belt, and shoulder belts was developed using the belt routing tool in LS-PrePost v4.9.12 (LS-PrePost, Livermore Software Technologies, Livermore, CA, USA).

This paper is a student paper from the 19th Injury Biomechanics Symposium and is published in a special issue of SAE International Journal of Transportation Safety.
It is preliminary work, has not been peer reviewed, and should not be cited because it is a work in progress.

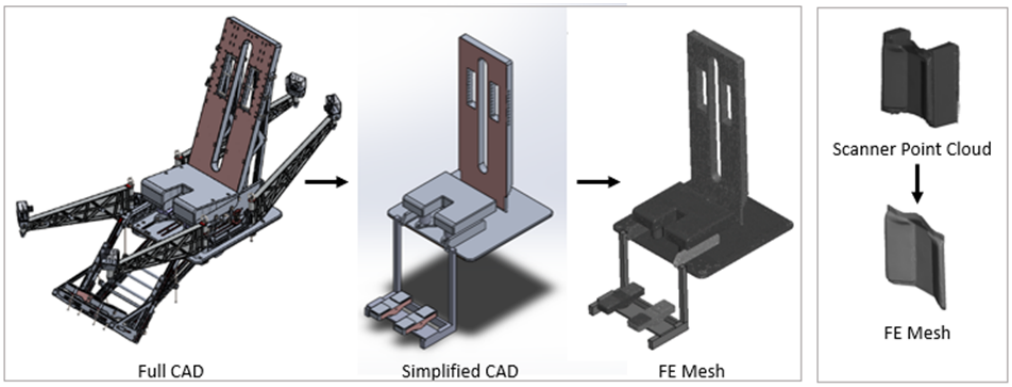

Figure 3: Process of seat fixture simplification from CAD and FE mesh generation.

The overall fixture and shoulder belt response was validated using ATD data from the same drop tower facility as part of a previous effort [DeWitt et al., 2023]. A brief summary of the results can be found in Appendix A. The THUMS model was positioned using Oasys Primer 18.1 (Primer, Oasys Ltd, Solihull, UK) with targets derived from the previously mentioned FARO point data. Anatomical landmarks included infraorbital notch, tragion, acromion, sternal notch, and greater trochanter (GT). X-ray images from testing were stitched and used to develop a target spine curvature corridor (Figure 4).

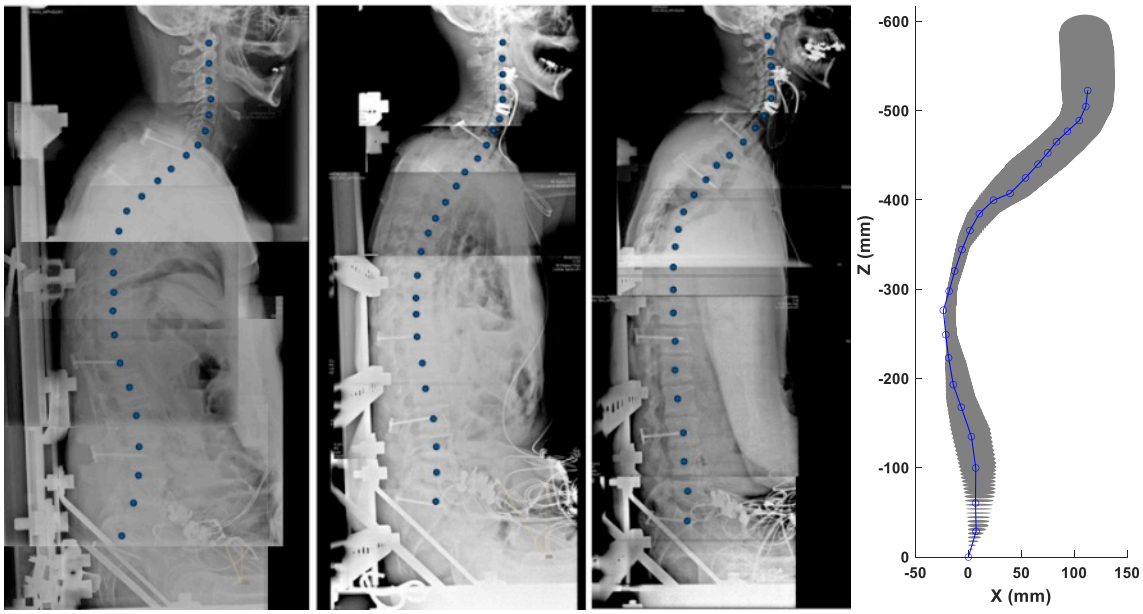

Figure 4: PMHS stitched X-rays, selected points at the approximate vertebral body center for spine curvature characterization and achieved THUMS spine curvature after positioning.

Once positioned, the updated THUMS model was settled into the seat in both the x- and z-direction using gravity simulations developed in LS-PrePost. To ensure no undesired changes in the HBM orientation, Boundary_SPC_Sets were used on the model skeleton to constrain the parts in all degrees of freedom other than the axis where settling was occurring. The harness and restraint

This paper is a student paper from the 19th Injury Biomechanics Symposium and is published in a special issue of SAE International Journal of Transportation Safety.
It is preliminary work, has not been peer reviewed, and should not be cited because it is a work in progress.

models were then manually adjusted to fit the position of the THUMS model using the Transform tool. The average acceleration pulse from the experimental data was used to drive the simulation using Boundary_Prescribe_Motion keyword assigned to the seat fixture floor. The Initial_Velocity keyword was also used on the entire setup to mimic the free fall experienced during the testing. Retractor elements in the harness and anchor locations for the shoulder and lap belts were allowed to pre-tension (89N) for 50ms before pulse initiation. A comparison of the model setup to the experimental setup for PMHS2 is shown in Figure 5. Positioning target information for the final setup is summarized in Table 1. Green in the THUMS position indicates an achieved position within one standard deviation of the average PMHS and red indicates that the THUMS position is outside of one standard deviation.

Table 1: Achieved THUMS position vs. PMHS average

	PMHS Average ± Standard Deviation		**THUMS Positions**	
	x (mm)	z (mm)	x (mm)	z (mm)
Right Acromion	212.6 ± 12.0	-497.7 ± 25.5	153.0	-498.0
Right GT	165.0 ± 5.4	-23.2 ± 11.1	166.2	-12.8
Sternal Notch	228.1 ± 10.8	-479.3 ± 23.5	198.2	-485.7
Right Infraorbital	303.9 ± 12.8	-679.8 ± 31.3	305.8	-666.1
Right Tragion	223.1 ± 10.8	-678.2 ± 31.1	217.7	-673.4

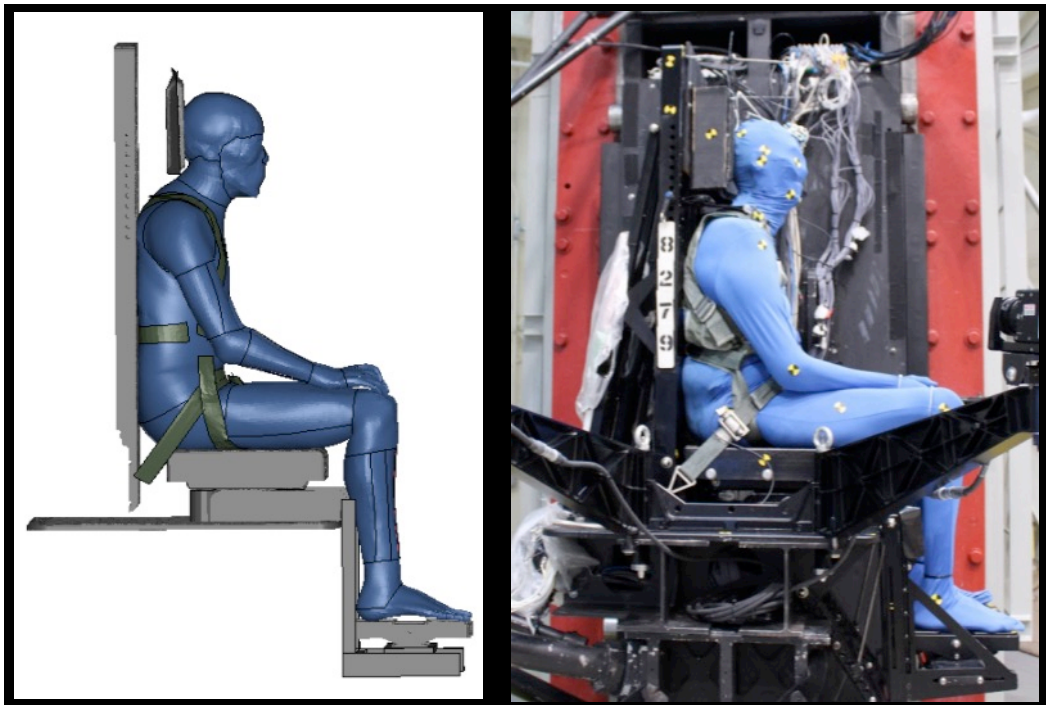

Figure 5: THUMS simulation setup (left) compared to experimental setup for PMHS2 (right).

This paper is a student paper from the 19th Injury Biomechanics Symposium and is published in a special issue of SAE International Journal of Transportation Safety.
It is preliminary work, has not been peer reviewed, and should not be cited because it is a work in progress.

A subset of anthropometric measurements for the three PMHS and the THUMS model are also presented in Table 2.

Table 2: Comparison of anthropometric measurements for PMHS and THUMS

Anthropometric Measurements						
Subject	**Height (cm)**	**Seated Height (cm)**	**Chest Circumference (cm)**	**Waist Circumference (cm)**	**Weight (kg)**	**BMI**
PMHS1	173.5	84.9	109.0	96.6	80.5	26.7
PMHS2	183.0	89.3	98.0	103.5	76.9	23.0
PMHS3	182.5	92.7	102.1	105.3	94.8	28.5
THUMS	173.0	88.2	95.3	83.0	77.3	25.8

To replicate the 6DOF instrumentation in the thoracic and lumbar spine during testing, local coordinate systems were defined on each of the vertebral bodies using Define_Coordinate_Nodes. Nodes used to define the local coordinate systems were constrained using Constrained_Interpolation, and nodal time-history outputs were recorded for a node on the anterior surface of the vertebral body using Database_History_Node_Local. To estimate the force in the intervertebral discs for comparison to experimental data the Database_Cross_Section_Set keyword was used. For the definition of the keyword, solid sets were defined using the central 3D elements of the intervertebral disc in the model and the nodes on the superior surface of those central elements for both the annulus fibrosis and nucleus pulposus. Examples of the instrumentation definitions are shown in Figure 6.

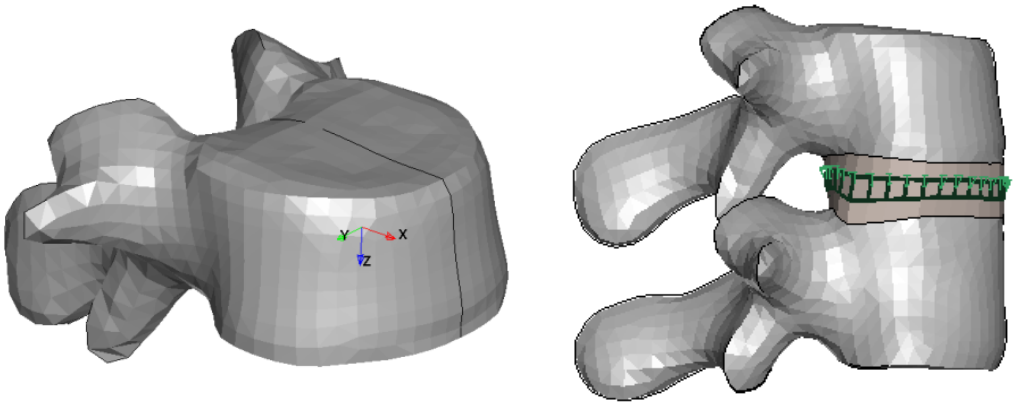

Figure 6: Local coordinate system for vertebral body kinematics (left) and location of intervertebral disc force measurement (right).

All simulation results were output at a frequency of 20,000 Hz to match the experimental setup. Post-processing of the data was performed the same as the PMHS; however, because of the predefinition of the anatomical coordinate system in the model, no coordinate system transformations were required.

This paper is a student paper from the 19th Injury Biomechanics Symposium and is published in a special issue of SAE International Journal of Transportation Safety.
It is preliminary work, has not been peer reviewed, and should not be cited because it is a work in progress.

Model Response Evaluation

All experimental data were imported into MATLAB, and a custom script was used to determine the average peak PMHS response and standard deviation. Corridors for local vertebral body z-axis acceleration and y-axis angular velocity were developed as well as corridors for lumbar spine force estimates for comparison to model response.

RESULTS

Simulations were successfully completed with normal termination. Qualitative kinematic comparison of model response to PMHS response using high-speed video showed similar trends between the two environments. Both PMHS and THUMS experienced cervical spine extension at the initial pulse onset followed by flexion. Torso compression between PMHS and THUMS corresponded with the peak acceleration; however, the magnitude of the compression was visibly higher in the THUMS model than in the PMHS. The overall kinematics for PMHS2 and THUMS are shown in Figure 7.

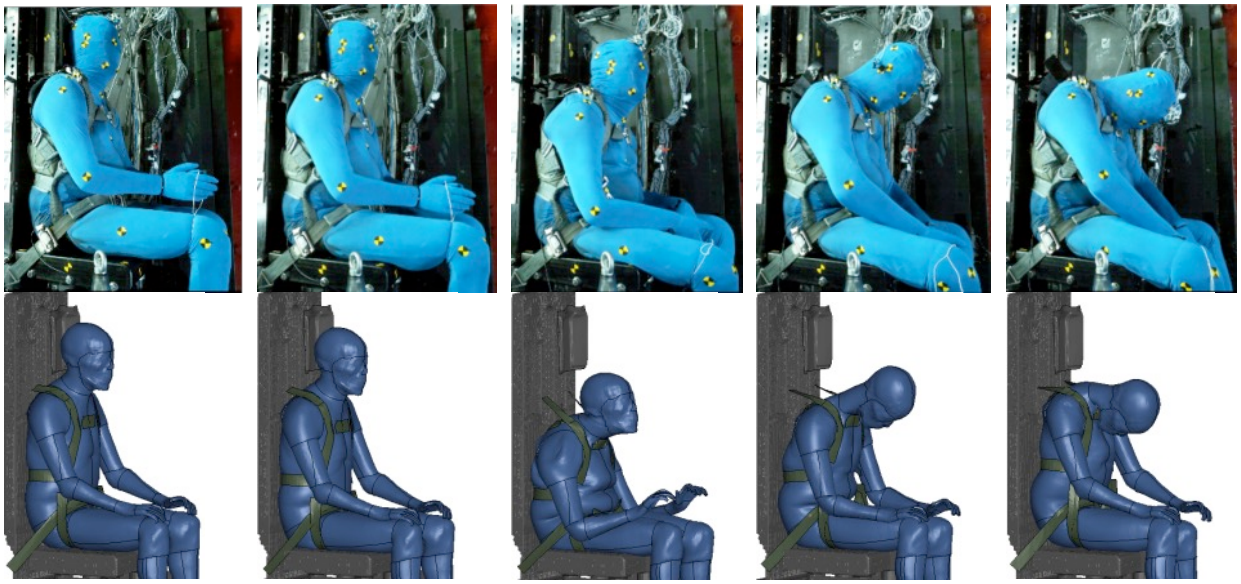

Figure 7: Still images from highspeed video for PMHS2 and THUMS showing occupant kinematics.

Seat pan force data from the PMHS testing were normalized to account for observed differences between PMHS weight and torso size (Table 2) before comparison to simulation results. Normalization was done using a ratio of torso volume between the THUMS model and PMHS using Equations 1-3. Simulation results showed a total seat reaction force of 12.7kN, which was within the range of the normalized experimental values (12.3kN to 13.2kN). The carriage acceleration for test and simulation as well as time history for seat forces are shown in Figure 8.

This paper is a student paper from the 19th Injury Biomechanics Symposium and is published in a special issue of SAE International Journal of Transportation Safety.
It is preliminary work, has not been peer reviewed, and should not be cited because it is a work in progress.

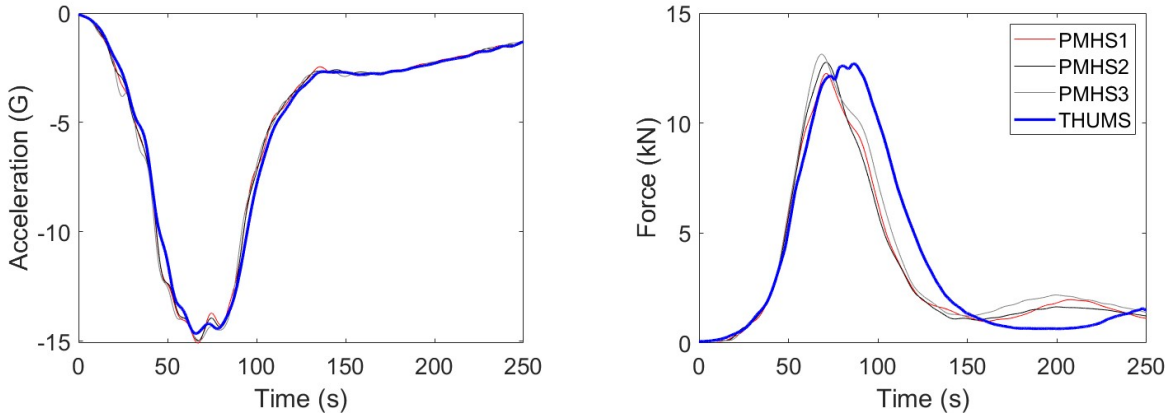

Figure 8: Carriage acceleration (left) and seat reaction force (right) from experiments and simulation.

Shoulder belt forces from the simulation were measured in the 1D belt elements connecting the harness to the fixture floor in a location similar to the physical location of the inline belt loadcells during testing. The average peak force for the THUMS model was 637.0N, which was within the experimental range observed during PMHS testing (462.2N to 703.3N).

$$F_n = F_{PMHS} * \frac{v_{THUMS}}{v_{PMHS}} \quad (1)$$

$$v = pi * r^2 * SH \quad (2)$$

$$r = \frac{CC + WC}{4 * pi} \quad (3)$$

Where:
F_n = normalized PMHS force
F_{PMHS} = measured PMHS force
v = estimated torso volume
r = estimated radius
SH = measured seated height
CC = measured chest circumference
WC = measured waist circumference

Simulation local z-axis linear acceleration showed good agreement at S1, L3, and T12, all falling within one standard deviation of the experimental values. T4 and T1 z-axis linear acceleration predicted by the simulation were well outside of the range recorded during testing. Time-history response data showed similar trends during initial acceleration onset followed by large signal spikes beginning at approximately 71ms and again at 145ms. These spikes also seem to correspond to rapid changes in the y-angular velocity measurements at these locations as well. Peak y-angular velocity measurements at all levels, however, were outside of the experimentally recorded values. Similar trends in the simulation results compared to PMHS can be seen during the initial 100ms of simulation, showing rearward rotation at S1 and L3, and forward vertebral body rotation at T12, T4, and T1. Peak response values, however, were often twice or more the

This paper is a student paper from the 19th Injury Biomechanics Symposium and is published in a special issue of SAE International Journal of Transportation Safety.
It is preliminary work, has not been peer reviewed, and should not be cited because it is a work in progress.

values recorded during testing. These results are summarized in Table 3, and time histories compared to experimental corridors are shown in Figures 9-12.

Table 3: Vertebral body kinematic summary for z-axis linear acceleration (G) and y-angular velocity (deg/s)

Instrumentation		PMHS Average ± Std Dev	THUMS
T1	**z-acceleration**	-17.9 ± 5.6	-97.6
	y-angular velocity max	559.8 ± 55.6	1920.9
	y-angular velocity min	-809.0 ± 288.3	-2006.1
T4	**z-acceleration**	-19.3 ± 3.4	-46.6
	y-angular velocity max	341.0 ± 30.1	937.1
	y-angular velocity min	-711.1 ± 115.0	-1608.2
T12	**z-acceleration**	-22.7 ± 1.9	-22.7
	y-angular velocity max	192.6 ± 174.8	773.7
	y-angular velocity min	-276.5 ± 68.6	-491.5
L3	**z-acceleration**	-26.6 ± 12.4	-21.8
	y-angular velocity max	173.1 ± 52.9	357.2
	y-angular velocity min	-86.3 ± 21.7	-489.5
S1	**z-acceleration**	-23.6 ± 7.1	-19.6
	y-angular velocity max	289.3 ± 4.4	581.2
	y-angular velocity min	-101.9 ± 12.2	-620.3

This paper is a student paper from the 19th Injury Biomechanics Symposium and is published in a special issue of SAE International Journal of Transportation Safety.
It is preliminary work, has not been peer reviewed, and should not be cited because it is a work in progress.

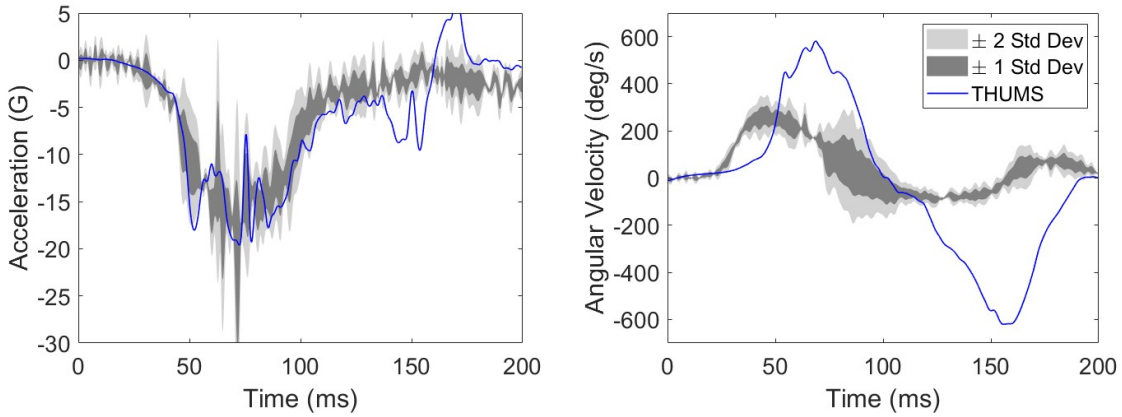

Figure 9: S1 z-acceleration (left) and y-angular velocity (right) THUMS response and experimental corridors.

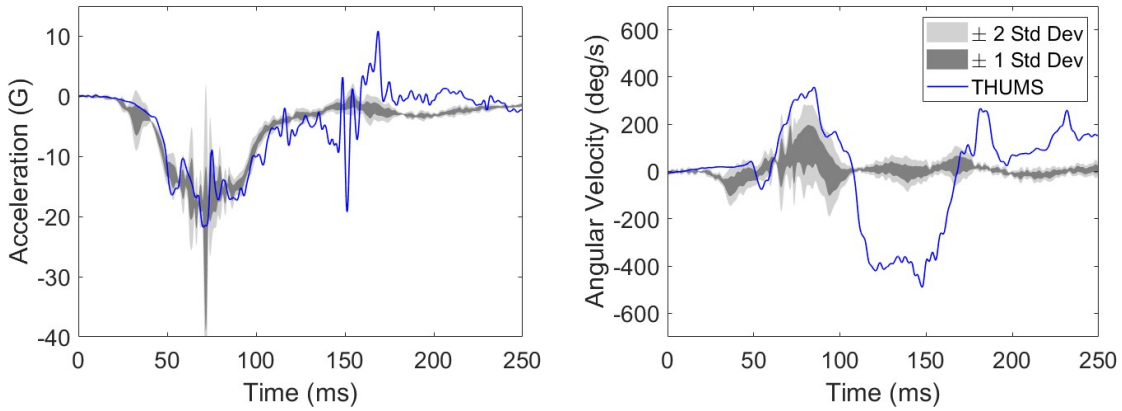

Figure 10: L3 z-acceleration (left) and y-angular velocity (right) THUMS response and experimental corridors.

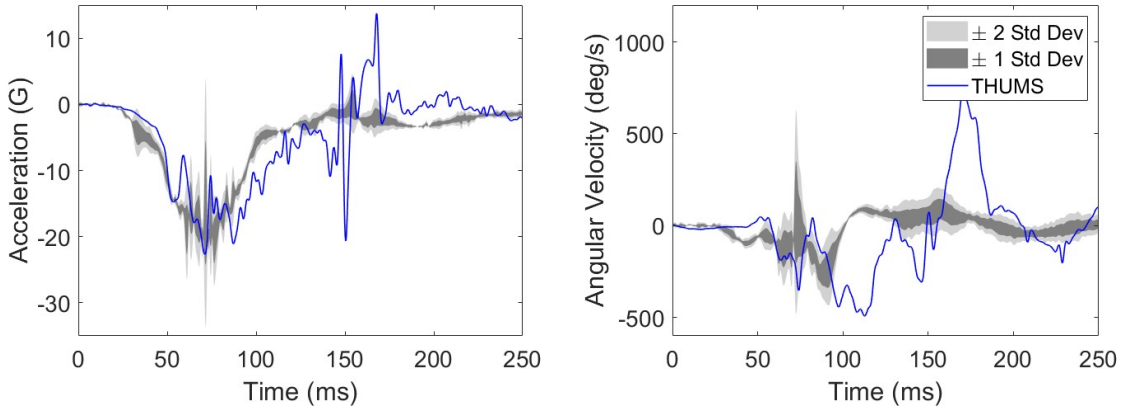

Figure 11: T12 z-acceleration (left) and y-angular velocity (right) THUMS response and experimental corridors.

This paper is a student paper from the 19th Injury Biomechanics Symposium and is published in a special issue of SAE International Journal of Transportation Safety.
It is preliminary work, has not been peer reviewed, and should not be cited because it is a work in progress.

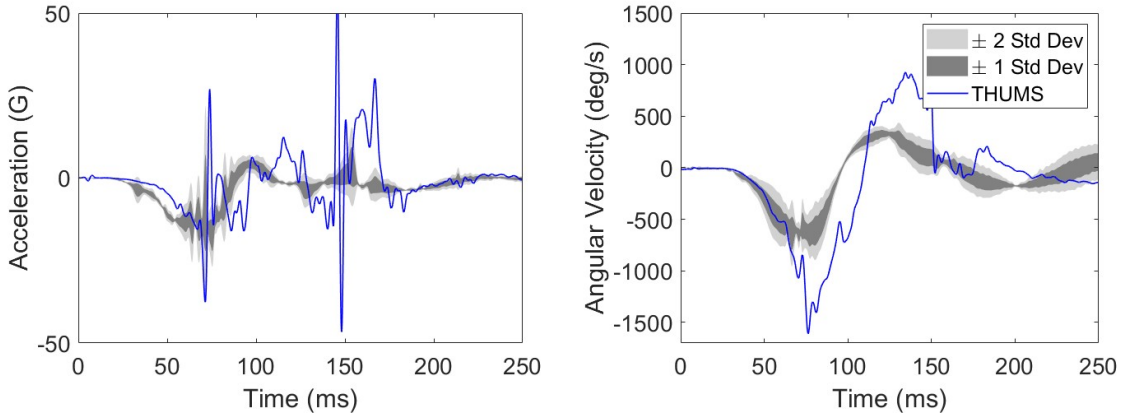

Figure 12: T4 z-acceleration (left) and y-angular velocity (right) THUMS response and experimental corridors.

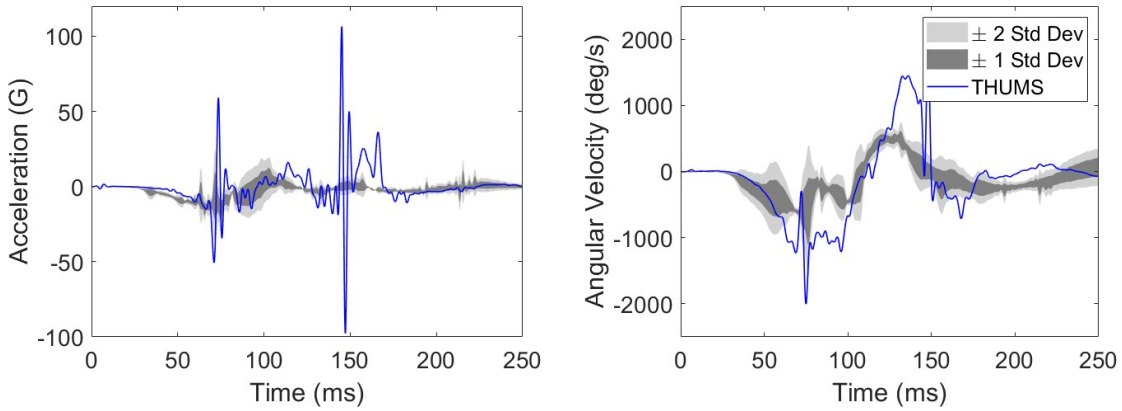

Figure 13: T1 z-acceleration (left) and y-angular velocity (right) THUMS response and experimental corridors.

An average response corridor was created using all the successfully recorded pressure data for all levels for comparison to the average THUMS model response. The average peak response in the simulation was -3.3kN, which was outside of two standard deviations from the experimental average (-6.9 ± 1.4kN). The peak response timing was also inconsistent with PMHS testing (Figure 14), with a noticeable phase shift of approximately 25ms from the experimental response.

This paper is a student paper from the 19th Injury Biomechanics Symposium and is published in a special issue of SAE International Journal of Transportation Safety.
It is preliminary work, has not been peer reviewed, and should not be cited because it is a work in progress.

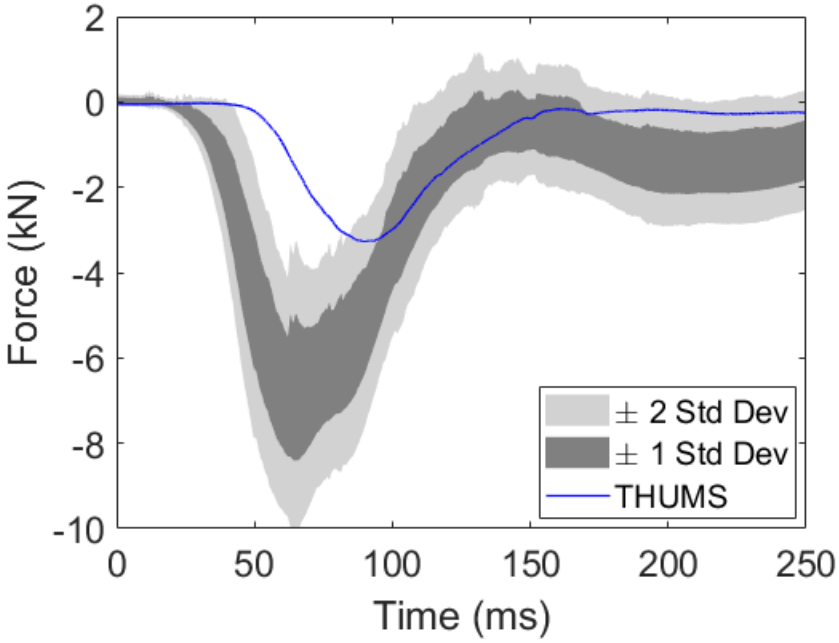

Figure 14: Average THUMS lumbar intervertebral disc force compared to PMHS corridors.

DISCUSSION

PMHS response data were successfully collected for three subjects. 6DOF measurements transformed to the local anatomical coordinate system of the PMHS provided a foundational data set for the development of response corridors for the THUMS model validation. Good agreement was found between PMHS and THUMS response for the local z-axis acceleration at S1, L3, and T12; however, notable differences were observed in z-axis accelerations of T4 and T1 as well as all y-angular velocity measurements recorded. Spikes were observed in the z-axis acceleration of T4 and T1, which contributed to the differences in reported peak values. While no visible contact between adjacent vertebral bodies was observed, the initiation of the signal disturbance seemed to correlate with adjacent bodies reaching peak relative flexion in both instances. Investigation into the angular displacement of each vertebral body that experienced the large accelerative spikes showed that the spikes corresponded with angular displacement limits and sharp fluctuation in angular displacement values. At the time the angular limit appeared to be reached, rapid oscillatory changes were observed before a smooth change in angular displacement direction was achieved. Further work should be done to understand contact definitions in the region and evaluate the effect of potential local damping on minimizing these disturbances in signal response.

Trends in polarity between PMHS response and THUMS with respect to angular velocity were similar, however, angular velocity data was overpredicted by THUMS at all levels. This could be indicative of a less stiff material model used to represent the material of the intervertebral disc in the THUMS model vs actual PMHS intervertebral disc stiffness. It should be noted, however, that initial spine curvature characterization was based on approximate vertebral body centers and not individual vertebral body angles. The initial orientation of the vertebral bodies with

This paper is a student paper from the 19th Injury Biomechanics Symposium and is published in a special issue of SAE International Journal of Transportation Safety.
It is preliminary work, has not been peer reviewed, and should not be cited because it is a work in progress.

respect to the PMHS should be further evaluated and a sensitivity study performed to see if the initial angle of the vertebral body significantly influences the observed angular velocity response at these levels.

Calculated lumbar force corridors from PMHS testing showed the THUMS model under-predicting total average force in the intervertebral discs of the lumbar spine. PMHS forces were estimated based on pressure changes in the intervertebral discs at a single location. Visible flexion determined by high-speed video and angular rate data on the S1 and L3 vertebral bodies was observed and has been reported to influence pressure sensor response in intervertebral discs (Demotropoulous et al., 2007). This could have contributed to the reported higher PMHS values for comparison. Demotropoulous et al. (2007) reported pressure changes in L3-L4 intervertebral discs as high as 51psi at 10Nm flexion moment. Multiple pressure sensors should be considered for future work to determine any variation of pressure within the intervertebral disc due this contribution. THUMS has the ability to report flexion/extension moments at the same locations as the force measurements were taken, and it experienced a peak flexion moment of approximately 12Nm at the time of the reported peak force. Assuming a similar moment was observed in the PMHS, this could account for an approximate 0.8kN increase in the calculated force values that were used to develop PMHS corridors. Further investigation was performed to evaluate the effects of using pressure recorded in intervertebral discs of the THUMS model and calculating peak force the same way performed for the PMHS. This resulted in an average peak force of 5.0kN for the THUMS model, which is within two standard deviations of the experimental average and 1.7kN higher than forces reported through the Database_Cross_Section. It should be noted, however, that this was performed using outputs from the D3plot files from simulation and were at much lower sampling frequency than the time history files. Increased frequency of the outputs for the pressure could result in higher reported peak values and should be considered for further evaluation. Additional work should be done to better quantify the moment effect on the PMHS lumbar force estimates before final validation of the FE HBM lumbar spine response is performed.

CONCLUSIONS

The study presented outlines methodologies to be used for the development of PMHS spine kinematic and lumbar force corridor development for future use in FE HBM validation to vertical loading. All findings are preliminary, and more work is needed to evaluate the experimental response data and determine appropriate boundary conditions for simulation before model validation. Three of six planned PMHS tests were completed and have shown success in generating useful data. However, more data are still needed to quantify subject response variation in this specific environment.

ACKNOWLEDGEMENTS

We would like to sincerely thank the anatomical donors of the Ohio State Body Donation program, who made this research possible. We would also like to thank all of the team members of the Injury Biomechanics Research Center who assisted with this test program and the members of the Air Force Research Labs who provided support during drop tower testing.

REFERENCES

Auffret R. “Spine Injury After Ejection.” Advisory Group for Aerospace Research and Development, 1975.

Collins R, McCarthy GW, Kaleps I, Knox FS. “Review of major injuries and fatalities in USAF ejections, 1981-1995.” Biomed Sci Instrum. 1997.

Decker W, Koya B, Pak W, Untaroiu C D, & Gayzik F S. “Evaluation of finite element human body models for use in a standardized protocol for pedestrian safety assessment.” Traffic Injury Prevention, 2019.

DeWitt T, Pradhan V, Kang YS. "Development and Validation of seat Fixture and Restraint Model for use in FE HBM Evaluation During Vertical Loading" IBS Conference, 2023.

DODIG-2015-090. “Evaluation of Aircraft Ejection Seat Safety When Using Advanced Helmet Sensors.”US Department of Defense Memorandum, 2015.

EZFC-CSB-16-001, Crew Systems Bulletin, “USAF Revision of MIL-HDBK-516C Section 9.1.1 Escape System Safety Compatibility Criteria Standard. Air Force Technical Bulletin, 2016.

Harper J. “Next-Generation Ejection Seats to Include New Safety Features.” National Defense Magazine, 15 Nov.2019.www.nationaldefensemagazine.org/articles/2019/11/15/next-generation-ejection-seats-to-include-new-safety-features.

Gepner B, Rapela D, Forman J, Ostling M, Pipkorn B, Kerrigan J. “Evaluation of GHBMC, THUMS and SAFER Human Body Models in Frontal Impacts in Reclined Postures.” IRCOBI Conference, 2022.

Katagiri M, Zhao J, Kerrigan J, Kent R, Forman J. “Comparison of Whole-Body Kinematic Behaviour of the GHBMC Occupant Model to PMHS in Far-Side Sled Tests.” IRCOBI Conference, 2016.

Mattock M, Asch B, Hosek J, Boito M. “Rand Corporation, The Relative Cost-Effectiveness of Retaining Versus Accessing Air Force Pilots.” Technical Report, 2019.

Parate B A, Arellano-Garcia H. “Science And Technology of Aircraft Seat Ejection: Advanced Concepts.” Cogent Engineering, 2022.

Pellettiere J, Desjardins S, Tulloch J. “Development of lumbar injury tolerance criteria.” Proceedings - Annual SAFE Symposium, 2013.

SAE International Surface Vehicle Recommended Practice, “Instrumentation for Impact Test – Part 1 – Electronic Instrumentation.” SAE Standard J211-1, Rev. Mar. 2014.

This paper is a student paper from the 19th Injury Biomechanics Symposium and is published in a special issue of SAE International Journal of Transportation Safety.
It is preliminary work, has not been peer reviewed, and should not be cited because it is a work in progress.

Slykhouse, L., Zaseck, L. W., Miller, C., Humm, J.R., Alai, A., Kang, Y. S., ... and Reed, M. P. "Anatomically-based skeletal coordinate systems for use with impact biomechanics data intended for anthropomorphic test device development." Journal of biomechanics, 2019.

Somers J, Gohmert D, Brinkley J. "Application of the Brinkley Dynamic Response Criterion to Spacecraft Transient Dynamic Events." NASA Technical Memorandum, 2013.

Thompson L. "Congress Should Fully Fund the Air Forces Long-Overdue Competition for a Safer Ejection Seat." Forbes, 15 July 2019.

Toyota Motor Corporation Documentation, Total Human Model for Safety, AM50 Occupant Model Version 6.1, 2021.

This paper is a student paper from the 19th Injury Biomechanics Symposium and is published in a special issue of SAE International Journal of Transportation Safety.
It is preliminary work, has not been peer reviewed, and should not be cited because it is a work in progress.

APPENDIX A

Three drop tower tests were successfully conducted to develop data for FE fixture and restraint validation. Comparison of high-speed video from testing and simulation outcomes showed similar ATD kinematics through the duration of the loading. Key events are shown in Fig. 10.

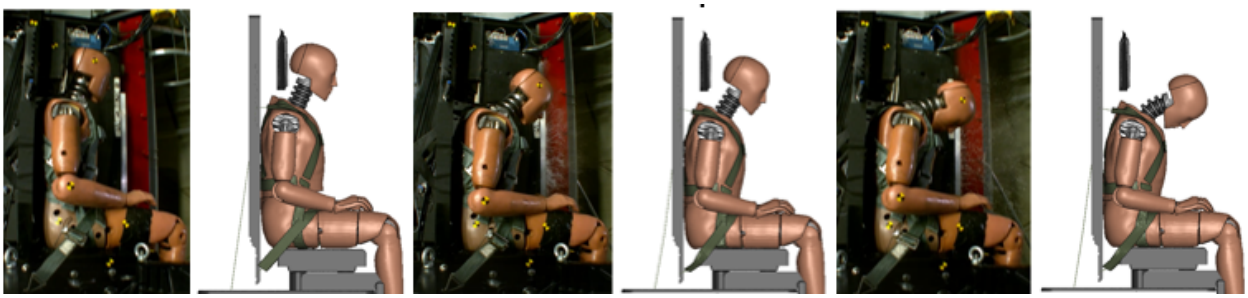

(a) (b) (c)

Fig. 15. High speed video and simulation comparison of ATD kinematics for initial state (a), peak pelvis compression (b) and peak neck flexion (c)

ATD testing showed good repeatability between the response parameters evaluated and is shown by the small calculated standard deviations between peak acceleration response values. Average NRMSD values comparing simulation responses were calculated and were within 8% for four of the five response variables of interest. Average NRMSD values for shoulder belt loads trended higher (14.3%) between simulation and experimental response however, greater variability was also observed in the shoulder belt loads during testing and the peak simulation response was still found to be within one standard deviation of the average peak for the experimentally recorded values. These findings are summarized in Table VI.

Table IV
Peak response data and calculated NRMSD values for fixture evaluation using ATD test data

Parameter	Peak Experimental Average and Standard Deviation	Peak Simulation	Average NRMSD (%)
Head Z Acceleration	15.2 ± 0.2G	15.7G	7.6
Chest Z Acceleration	17.9 ± 0.3G	18.5G	7.0
Pelvis Z Acceleration	16.8 ± 0.1G	17.0G	7.8
Seat Load	13.4 ± 0.1kN	14.2kN	6.5
Shoulder Belt Load	368.5 ± 53.6N	319.7N	14.3

This paper is a student paper from the 19th Injury Biomechanics Symposium and is published in a special issue of SAE International Journal of Transportation Safety.
It is preliminary work, has not been peer reviewed, and should not be cited because it is a work in progress.